

Synthetic 2-D Lead Tin Sulfide Nanosheets with Tuneable Optoelectronic Properties from a Potentially Scalable Reaction Pathway

Kane Norton,^{a†} Jens Kunstmann,^{b†*} Lu Ping,^a Alexander Rakowski,^c Chuchen Wang,^a Alexander J. Marsden,^d Ghulam Murtaza,^b Niting Zeng,^a Simon J. McAdams,^{a,c} Mark A. Bissett,^{a,d} Sarah J. Haigh^{a,d} Brian Derby,^a Gotthard Seifert,^b and David J. Lewis^{a*}.

^a*School of Materials University of Manchester, Oxford Road, Manchester, United Kingdom, M13 9PL.*

^b*Theoretische Chemie, Technische Universität Dresden, 01069 Dresden, Germany*

^c*School of Chemistry, University of Manchester, Oxford Road, Manchester, United Kingdom, M13 9PL.*

^d*National Graphene Institute, University of Manchester, Oxford Road, Manchester, United Kingdom, M13 9PL.*

Experimental Section

General Considerations. All chemicals and were purchased from Sigma Aldrich and used without further purification. All chemical reactions were performed in a nitrogen environment using standard Schlenk techniques.

Instrumentation. Scanning Electron Microscopy (SEM) was performed using a Zeiss Sigma VP instrument. Powders were mounted on stubs using Leit carbon tabs and were coated with carbon using an Edwards coater. Silver paint was also used to improve conductivity. EDX spectroscopy was performed in the SEM using an Oxford Instruments EDX detector. Powder X-ray diffraction (pXRD) was performed using a Bruker D8 Advance diffractometer using Cu K α (1.5406 Å) source was used to scan the samples. X'pert HiScore software was utilized to match the obtained patterns against known standard patterns. Raman microscopy was performed using a Renishaw 1000 microscopy system supplied with a 100 \times objective, the solid-state laser excitation length is 514 nm with 1% power and the diode laser source is 41.2 mW. A set point of 15-20 nm was used. HAADF STEM was performed using an FEI Titan ChemiSTEM 80-200 G2 probe side aberration corrected TEM fitted with a Super-X EDX detector. Samples were prepared by drop casting 5 \times 2 μ L drops of colloids onto a copper Quantifoil grid. Atomic force microscopy (AFM) was performed using a JPK nanowizard 4 AFM used

in AC tapping mode and equipped with Bruker TESPA V2 tips. Samples for AFM were prepared on Si/SiO₂ substrates; 5 drops of the dispersion were added to NMP using a glass dropper pipette, the samples were spin coated using an osilla spin coater at 6000 rpm for 60 seconds. These were then rinsed using 5 ml IPA and 5 ml deionised water and were then dried in a vacuum oven at 50 °C before analysis.

Synthesis of [Pb(S₂CNEt₂)₂](1). Sodium diethyl dithiocarbamate (5.0 g, 0.02 mol) in methanol (150 mL) was added drop-wise into a stirred solution (100 mL) of lead nitrate [Pb(NO₃)₂] (3.7 g, 0.01 mol) in methanol (100 mL). The reaction mixture was stirred at room temperature for another 30 minutes. The resulting suspension was filtered and washed with methanol (150 ml) to obtain a white solid which was dried under vacuum (3.6 g, 91%); mp 89-91 °C, FT-IR (ν_{\max} cm⁻¹): 2972(w), 1519(s), 1455(s), 1433(s), 1377(s), 1353(s), 1276(s), 1205(s), 1155(s), 1094(s), 1077(s), 992(s), 850(s), 781(s) Anal. Calc. for C₁₀H₂₂N₂S₄Pb: C, 23.75; H, 4.38; N, 5.54; S, 25.36; Pb, 40.97%. Found: C, 23.93; H, 4.46; N, 5.61; S, 25.55; Pb, 41.32 %.

Synthesis of [Sn(S₂CNEt₂)₂Bu₂](2). Sodium diethyl dithiocarbamate (5.0 g, 0.02 mol) in methanol (150 mL) was added drop-wise into di-n-butyl tin dichloride (3.4 g, 0.01 mol) in methanol (100 mL) with constant stirring. White precipitates of sodium chloride appeared which were removed by vacuum filtration after the addition was complete. The methanol was removed from the filtrate *in vacuo* at 40 °C. The white solid was purified by recrystallization from an ethanol chloroform mixture (1:1) and colourless crystals were collected (4.5 g, 77%). mp, 57-58 °C. FT-IR (solid) ν_{\max} /cm⁻¹: 2954 (w), 2925 (w), 1482 (m), 1457 (m), 1417 (s), 1352 (m), 1297 (m), 1252 (m), 1296 (m), 1205 (m), 1136 (s). Anal. Calc. for C₁₈H₃₈N₂S₄Sn: C, 40.86; H, 7.24; N, 5.29; S, 24.17 %. Found: C, 39.42; H, 7.92; N, 4.92; S, 22.93 %.

Synthesis of Bulk Powders by Melt Thermolysis. Melt reactions were performed by placing pre-mixed precursors at the appropriate stoichiometric ratios in a ceramic boat under a stream of argon (300 cm³ min⁻¹), in a Carbolite MTF 12/25/250 tube furnace which was then heated to 450 °C at a ramp rate of 20 °C min⁻¹ and was held at this temperature for 1 hour before being cooled to room temperature to furnish the Pb_xSn_{1-x}S solid state products.

Liquid Phase Exfoliation. Pb_{1-x}Sn_xS powders (120 mg, where x = 0.6, 0.8 and 1.0) were added to degassed NMP (5 mL). The suspension was ultrasonicated in an Elmasonic P bath operating at 37 kHz frequency and 30% power for 24 h. The bath was modified with water-cooling coil to maintain the water temperature below 30 °C. Upon completion of the exfoliation step, an aliquot (5 mL) was

removed to a centrifuge tube and diluted with NMP (5 mL). The dispersions obtained were centrifuged at 1500 rpm using a Thermo Heraeus MultifugeX1 for 45 min to separate the exfoliated nanosheets from remaining bulk material. After centrifugation, the top two-thirds of the solution were collected and drop casted onto glass slides (ultrasonically cleaned in acetone prior to deposition) and the solvent evaporated at 60 °C on a hotplate. For AFM, the glass slides were replaced by Si@SiO₂ substrates.

Theoretical Calculations. Pb_{1-x}Sn_xS crystals in monolayer, bilayer and bulk form were analysed with density functional theory (DFT) calculations using the Perdew–Burke–Ernzerhof (PBE) functional¹ and the Tkatchenko–Scheffler dispersion-interaction-correction scheme.² Band gaps were calculated with the Heyd-Scuseria-Ernzerhof-06 hybrid (HSE06) functional.^{3,4} For electronic structure analysis spin–orbit interactions were taken into account. We employed the projector augmented wave method⁵ and a plane-wave basis set with a cutoff energy of 259 eV (363 eV for cell optimizations), as implemented in VASP (Vienna Ab initio Simulation Package, version 5.4.4).^{6,7} The k-space integration was carried out with a Gaussian smearing method using an energy width of 0.05 eV. For the k-point sampling Γ -point-centred regular grids were used and the k-point density was converged such that total energy differences were smaller than 1 meV per atom. For compositions $x = 0$ or 1 calculations were done in the primitive unit cells shown in Fig. 1 of the main article and the k-meshes were 6×6×1 for monolayers and bilayers, 7×6×4 for orthorhombic bulk systems and 10×10×10 for cubic bulk systems. For alloys ($x \neq 0$ or 1) appropriate supercells were constructed (see Fig. S1) and the k-point meshes were reduced to achieve the same sampling density as for the primitive unit cells. Unit cells of monolayers and bilayers were built with 12 Å separation between replicates in the perpendicular direction to achieve negligible interaction. All systems were fully structurally optimized until all interatomic forces and stresses on the unit cell were below 0.01 eV Å⁻¹ and 10 kbar, respectively.

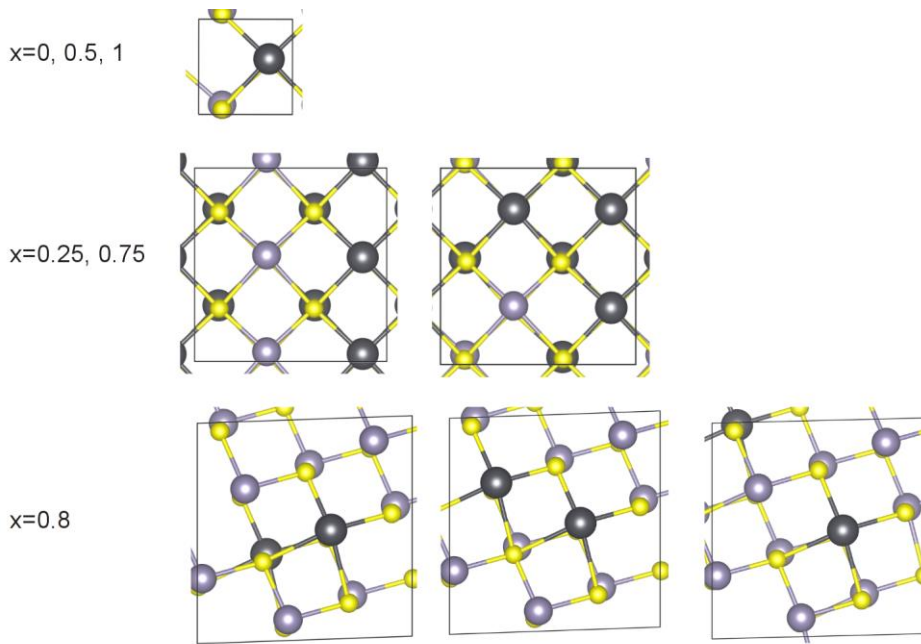


Figure S1: Atomic structures of monolayers of $\text{Pb}_{1-x}\text{Sn}_x\text{S}$ alloys as used in the DFT calculations. Unit cells are shown as black lines, bonds are drawn between nearest neighbor atoms (they do not necessarily represent covalent bonds), yellow, light gray and dark gray balls represent sulfur, tin and lead atoms, respectively. For $x=0, 0.5, 1$ the calculations are done in primitive unit cells with different atomic decorations, as shown for the case $x=0.5$ in the top line. For $x=0.25, 0.75, 0.8$ supercells were used (second and third line). For these systems the chemical composition x can be realized by multiple atomic configurations. We did not observe a strong dependence of structural, thermodynamic and electronic properties on specific configurations. Specifically for $x=0.8$ the three configurations gave very similar results. Calculations of bilayers and bulk were done using equivalent layers that are rotated relative to each other by 180 degrees according to the ABAB... stacking order in bulk.

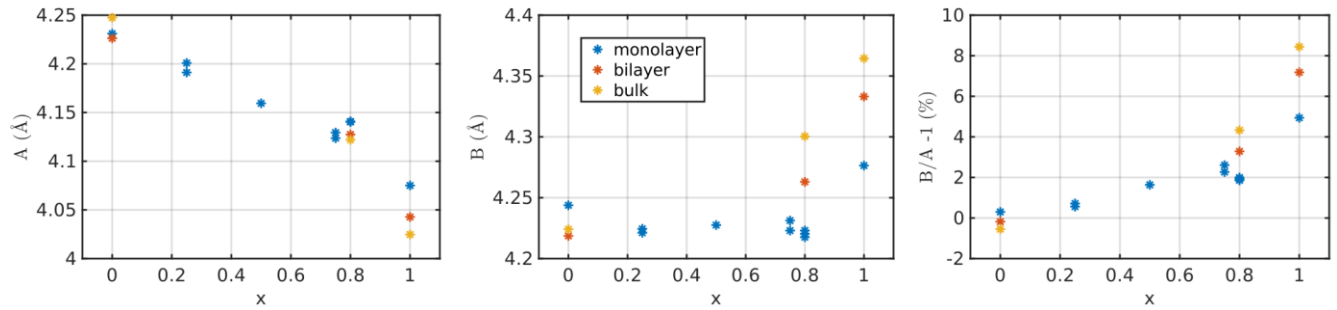


Figure S2: Structural changes in layered $\text{Pb}_{1-x}\text{Sn}_x\text{S}$ alloys as function of x , as calculated with DFT/PBE. Left: the in-plane lattice parameter A . Center: the in-plane lattice parameter B . Right: the relative difference of the lattice parameters (lattice anisotropy). For $x=1$ (SnS) the lattice anisotropy is ca. 8% for bulk but only 5% for a monolayer. This indicates that in SnS interlayer interactions lead to strong structural changes. For $x=0.8$ the lattice anisotropy is 4% and 2% for bulk and monolayers, respectively. This shows that alloying also induces strong structural changes. They are most pronounced for large x values. For small x the in-plane structure is almost isotropic, i.e., $A \approx B$. This is consistent with the stronger ionic character of the bonding in PbS . While the lattice parameter A changes almost continuously as function of x , B changes the most for large x values and little otherwise.

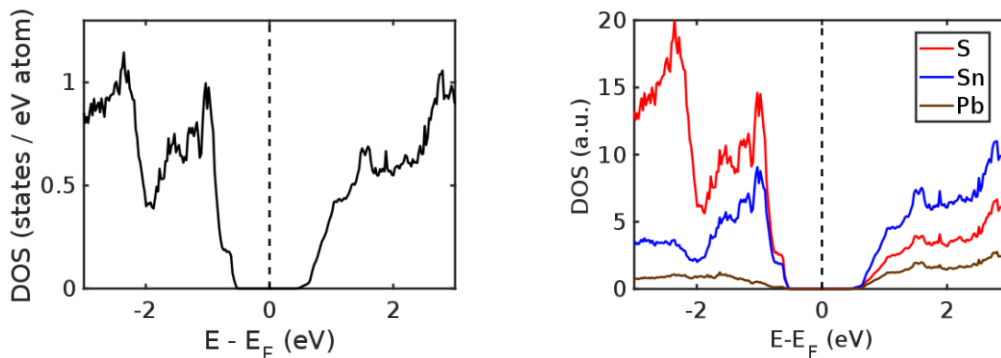


Figure S3: Density of states of bulk $\text{Pb}_{0.2}\text{Sn}_{0.8}\text{S}$ relative to the Fermi energy (E_F) as calculated with DFT/PBE. Left: total density of states (DOS). Right: atom-resolved projected DOS. The plot shows that the electronic states near the valence and conduction band edges are predominantly coming from S and Sn atoms; Pb atoms do not significantly contribute.

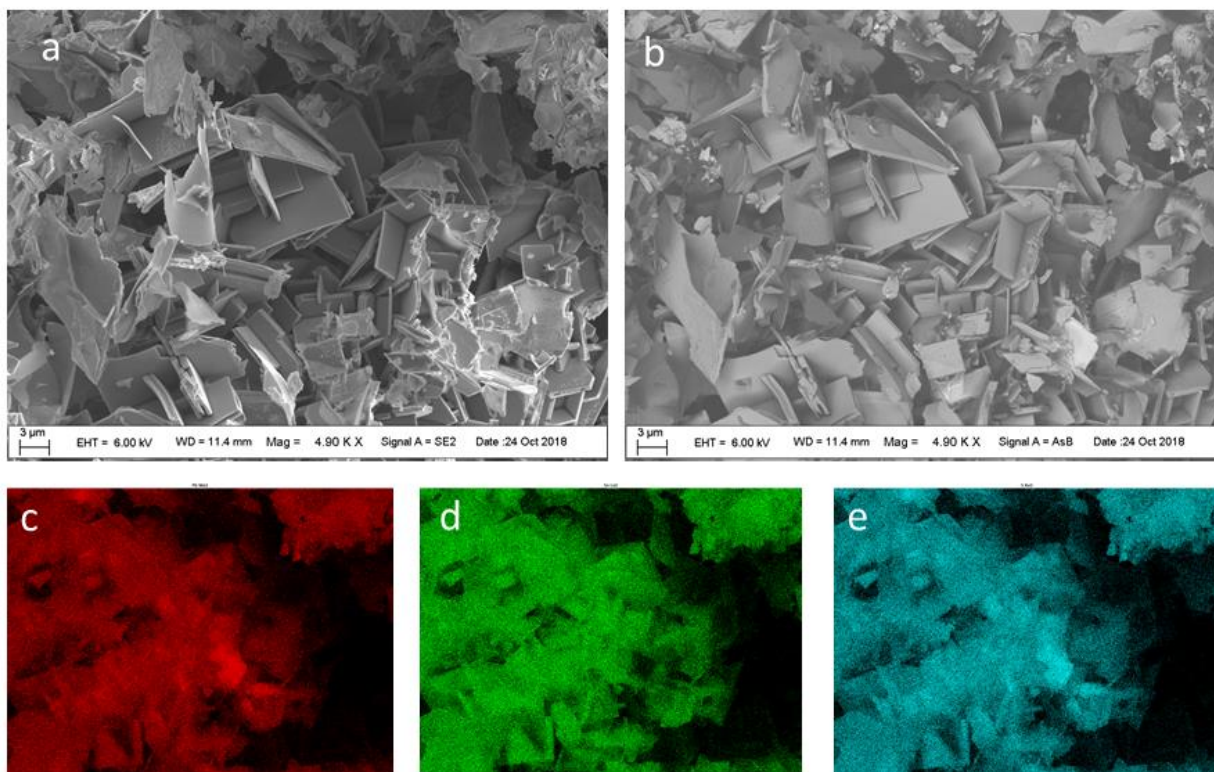


Fig S4: Characterisation of crystallites in $\text{Pb}_{0.2}\text{Sn}_{0.8}\text{S}$ by SEM and EDX spectrum mapping. (a) SE SEM image showing the appearance of the platy crystals suggestive of the orthorhombic structure observed in the PXRD pattern. (b) BS image of the same area as in (a), showing the z-contrast uniformity of the sample. (c) EDX spectrum map of the Pb $M\alpha$ emission line in the same area as in (a). (d) EDX spectrum map of the Sn $L\alpha$ emission line in the same area as in (a). (e) EDX spectrum map of the S $K\alpha$ emission line in the same area as in (a).

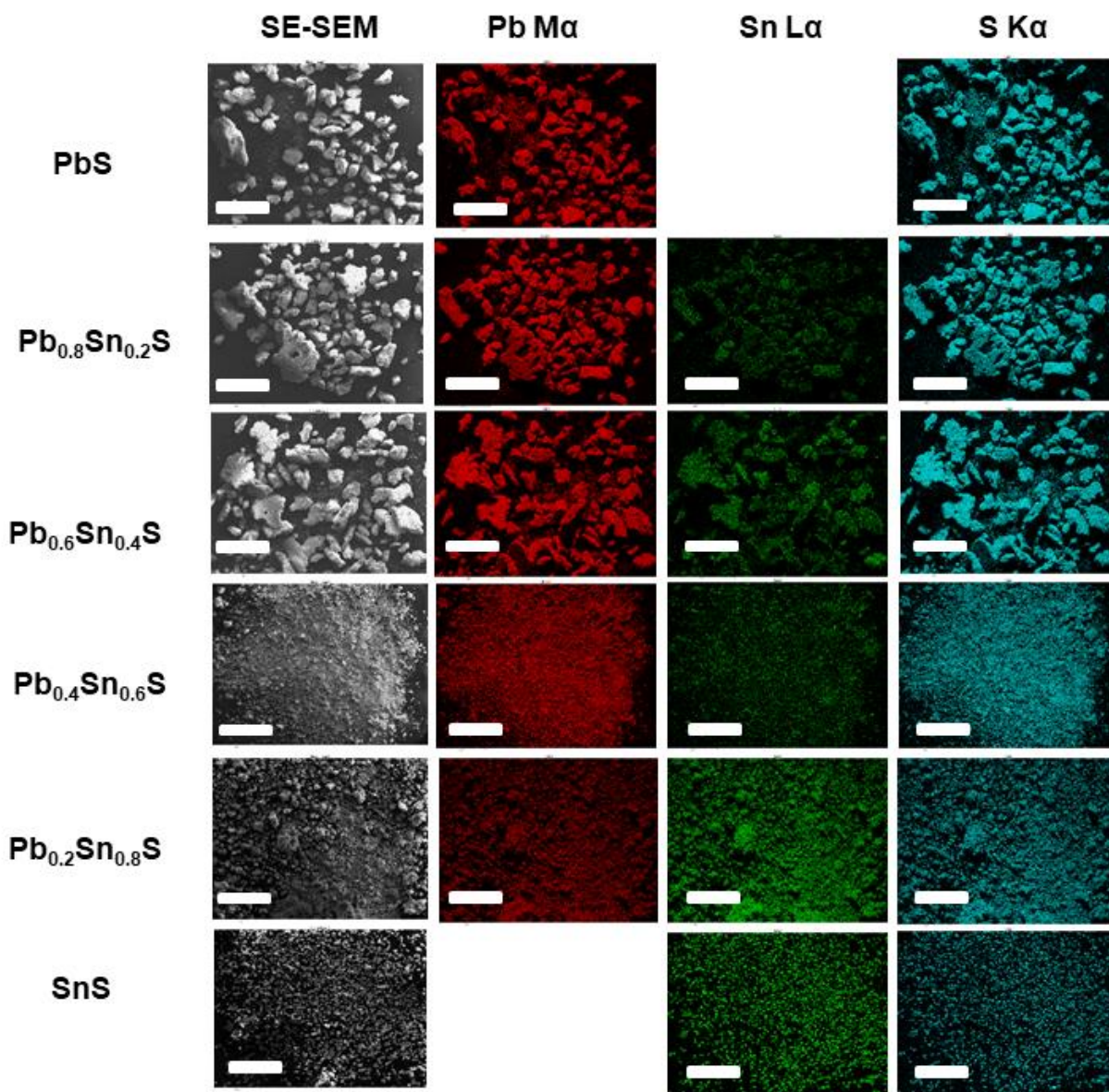


Figure S5: Wide area SE SEM images and EDX spectrum maps of PbSnS alloys. Scale bars represent 1 mm in all cases, apart from the SnS row where the scale bar represents 500 μm .

Supplementary References

1. J. P. Perdew, K. Burke and M. Ernzerhof, *Phys. Rev. Lett.*, 1996, **77**, 3865-3868.
2. A. Tkatchenko and M. Scheffler, *Phys. Rev. Lett.*, 2009, **102**, 073005.
3. J. Heyd, G. E. Scuseria and M. Ernzerhof, *J. Chem. Phys.*, 2003, **118**, 8207-8215.
4. J. Heyd, G. E. Scuseria and M. Ernzerhof, *J. Chem. Phys.*, 2006, **124**, 219906.
5. P. E. Blöchl, *Phys. Rev. B*, 1994, **50**, 17953-17979.
6. G. Kresse and J. Furthmüller, *Comp. Mater. Sci.*, 1996, **6**, 15-50.
7. G. Kresse and D. Joubert, *Phys. Rev. B*, 1999, **59**, 1758-1775.

